Downloaded from http://polymerphysics.net

Reinforcement Effect of Carbon Nanofillers in an Epoxy Resin System: Rheology, Molecular Dynamics, and Mechanical Studies

R. KOTSILKOVA,[1] D. FRAGIADAKIS,[2] P. PISSIS[2]

[1]Central Laboratory of Physico-Chemical Mechanics, Bulgarian Academy of Sciences, Academician G. Bonchev Street, Block 1, BG 1113 Sofia, Bulgaria

[2]Department of Physics, Zografou Campus, National Technical University of Athens, GR 15780 Athens, Greece

Received 28 February 2004; revised 8 September 2004; accepted 3 October 2004
DOI: 10.1002/polb.20352
Published online in Wiley InterScience (www.interscience.wiley.com).

ABSTRACT: The reinforcing effect of carbon nanoparticles in an epoxy resin has been estimated with different approaches based on rheology, molecular dynamics (evaluated by differential scanning calorimetry, dielectric relaxation spectroscopy, and thermally stimulated depolarization current), and dynamic mechanical analysis. Carbon particles aggregate as the volume increases and form a fractal structure in the matrix polymer. The dispersion microstructure has been characterized by its viscoelastic properties and relaxation time spectrum. The scaling of the storage modulus and yield stress with the volume fraction of carbon shows two distinct exponents and has thus been used to determine the critical carbon volume fraction of the network formation (Φ^*) for the carbon/epoxy dispersions. At nanofiller concentrations greater than Φ^*, the overall mobility of the polymer chains is restricted in both dispersions and solid nanocomposites. Therefore, (1) the relaxation spectrum of the dispersions is strongly shifted toward longer times, (2) the glass-transition temperature is increased and (3) the relaxation strength of both the secondary (β) and primary (α) relaxations increases in the nanocomposites, with respect to the pure polymer matrix. The dispersion microstructure, consisting of fractal flocs and formed above Φ^*, is proposed to play the main role in the reinforcement of nanocomposites. Moreover, the network structure and the interface polymer layer (bond layer), surrounding nanoparticles, increases the relaxation strength and slows the cooperative α relaxation, and this results in an improvement of the mechanical properties. © 2005 Wiley Periodicals, Inc. J Polym Sci Part B: Polym Phys 43: 522–533, 2005

Keywords: carbon nanoparticles; epoxy resin; dispersions; viscosity; viscoelastic properties; critical filler concentration; nanocomposites; molecular dynamics; dynamic mechanical properties; relaxation; reinforcement

INTRODUCTION

The inclusion of conductive nanoparticles, such as carbon in an insulating polymer, is usually used to take advantage of the improved conductivity of the polymer.[1] In our previous studies, we have used carbon nanofillers synthesized by a shock-wave method, and we have studied in detail the electrical and microwave-absorbing properties of composites based on thermosetting polymers.[2–4] The physical properties exhibited by such composites depend strongly on the microstructure of the dispersions. However, it is important for var-

Correspondence to: R. Kotsilkova (E-mail: kotsil@clphchm.bas.bg)

Journal of Polymer Science: Part B: Polymer Physics, Vol. 43, 522–533 (2005)
© 2005 Wiley Periodicals, Inc.

ious applications to study the reinforcement effect of nanofillers in polymer matrices to understand the mechanism of the improvement of the mechanical properties.

Different approaches have been proposed to investigate the effects of nanofillers, but we stress here the rheology, molecular dynamics, and dynamic mechanical studies. Rheology has been used as a tool for the characterization and control of the dispersion microstructure of fine particles within the liquid matrix. For colloidal dispersions, a cluster aggregation is proposed in which many particles diffuse and stick together to form clusters that also diffuse and stick. It has been shown recently that the two most popular models proposed for understanding colloidal aggregation, the diffusion-limited aggregation model and the cluster–cluster aggregation model, produce ramified structures that are self-similar and are known as fractals.[5–13] Power-law behavior as a function of the volume fraction usually shows that the aggregates are fractal. Although there have been many studies on the scaling (power-law) behavior of the rheology of colloidal dispersions,[10–14] polymer matrix nanodispersions have been explored less. Pelster and Simon[10] reported that a small increase in the filler loading in nanodispersions dramatically changed the interparticle distance and affected the degree of order. We have reported a correlation between the structures of nanodispersions and the specific properties of composite systems, such as the conductivity and microwave absorption.[2] In this article, we provide some examples to illustrate the application of rheology to the study of interactions in concentrated dispersions of carbon nanoparticles in an epoxy resin (ER) matrix.

Polymer dynamics have been investigated actively to evaluate the effects of interfaces in nanocomposites.[15–21] Because of the large surface areas of nanoparticles, the interfacial layer can represent a significant volume of the polymer and thus determine the properties of the material. The local chain dynamics and cooperative motion, affected by nanofillers embedded in a polymer matrix, have been studied recently with different techniques. In general, two effects contribute to changes in the overall molecular mobility in nanocomposites: (1) the loosened molecular packing of polymer chains due to the presence of nanoparticles and interactions with them, leading to increased free volume and enhanced molecular mobility, and (2) the formation of a layer of a modified polymer (bound polymer) around the nanoparticles, leading to decreased molecular mobility.[17] In our previous studies, we have used broadband dielectric relaxation spectroscopy (DRS) and have reported that the large-scale heterogeneity of the matrix is suppressed in nanocomposites and replaced by small-scale heterogeneity related to the presence of nanofillers.[19,21] In this study, we apply broadband DRS, thermally stimulated depolarization current (TSDC) measurements, and differential scanning calorimetry (DSC) to study molecular mobility in nanocomposites altered by the surfaces and aggregation of nanoparticles.

The reinforcement effect of nanofillers in polymers has been reported as a remarkable combination of high stiffness and toughness; this is in contradiction to conventional composites.[22–35] This synergy is probably caused by changes in the morphology of the polymer matrix due to the presence of nanofillers. There is not yet a satisfactory theoretical explanation for the origin of mechanical property improvements in polymer nanocomposites; however, it is generally agreed that the large surface-to-volume ratio of the nanoscale inclusions plays a significant role.[22–24] Two concepts are discussed in the literature. One assumes that the formation of a nanostructured network of finely dispersed particles, which are strongly bonded to the polymer, is probably responsible for the reinforcement. For the strongly aggregated systems, a complex inorganic structure has been proposed to be more effective in load-transfer mechanisms than a simple sphere.[27,28] In the other concept,[24–26] the existence of an interphase is integrated into a mechanical approach to describe the observed reinforcement in composites. Although some doubts remain about its physical existence, the interphase appears as a concept that takes into account the important modulus difference between the filler and polymer matrix above the main relaxation temperature of well-dispersed composite systems.[25–31]

To estimate the reinforcement effects of nanoparticles, we have investigated dispersions and solid nanocomposites of carbon in ER. We stress the rheological characterization of semiconcentrated and concentrated carbon/epoxy dispersions to evaluate the transition of the structure from an aggregated type to a network (fractal) type. Furthermore, the molecular dynamics and mechanical properties of solid composites are correlated with respect to the dispersion microstructure.

EXPERIMENTAL

Materials and Sample Preparation

The materials studied in this work consist of ER composites containing nanosized carbon particles (NCPs). The nanofiller component was supplied by the Materials Science Laboratory of the Space Research Institute (Bulgarian Academy of Sciences, Sofia, Bulgaria) and was synthesized by a shockwave propagation method.[36] The carbon nanofiller (NCPs) was synthesized as a mixture of disordered graphite and diamond in a 67:33 ratio, with a specific surface area (S) of 590 m^2/g (Blein method) and a specific gravity (ρ) of 1.86 g/cm^3. The diamond nanoparticles, with S = 230 m^2/g and ρ = 3.36 g/cm^3, could be separated from the NCP mixture with chemical purification. Obviously, the diamond particles in the NCP mixture were larger than the disordered graphite. Figure 1(a) presents a scanning electron micrograph of NCPs (data from ref. 37). Small inclusions (composed of diamond and graphite particles) are visible, with an average diameter of approximately 10 nm and a maximum diameter of approximately 50 nm. They formed large clusters of 200–1200 nm. Figure 1(b) compares the X-ray diffraction (XRD) spectra of NCPs and diamond nanoparticles. NCP XRD data show one peak for graphite (at 26.8°) and two peaks for diamond (at 43.5 and 75.7°) corresponding to d values of 3.32, 2.08, and 1.26 Å, respectively. This confirms the crystalline forms of the diamond particles and the amorphous forms of the graphite particles. Both XRD data and S values led to the conclusion that the diamond nanoparticles (~10 nm) were larger than the graphite (~3 nm). Araldite LY556 (bisphenol A epoxy resin; Ciba), with a viscosity (η) of 25 Pa s, was used as a matrix polymer.

Semidiluted and concentrated dispersions of 1–10 vol % NCP were prepared as the desired amount of the carbon nanoparticles was dispersed in the ER matrix by a high-power ultrasonic disperser. The carbon particle surfaces were negatively charged, as already reported in ref. 1. Thus, the NCP clusters were easily dispersed in a low polar epoxy matrix, and this led to a stable dispersion. However, we did not expect all the clusters of carbon powder to be broken down to single nanoparticles in ER, as the resulting dispersion was not transparent. Samples of solid composites (1–6 vol %) were prepared as diethylenetriamine in stoichiometric proportions was added to the dispersions as a hardener, and they were cured for 1 h at room temperature; this was followed by postcuring for 3 h at 140 °C. Table 1 presents the compositions and characteristic parameters of the samples.

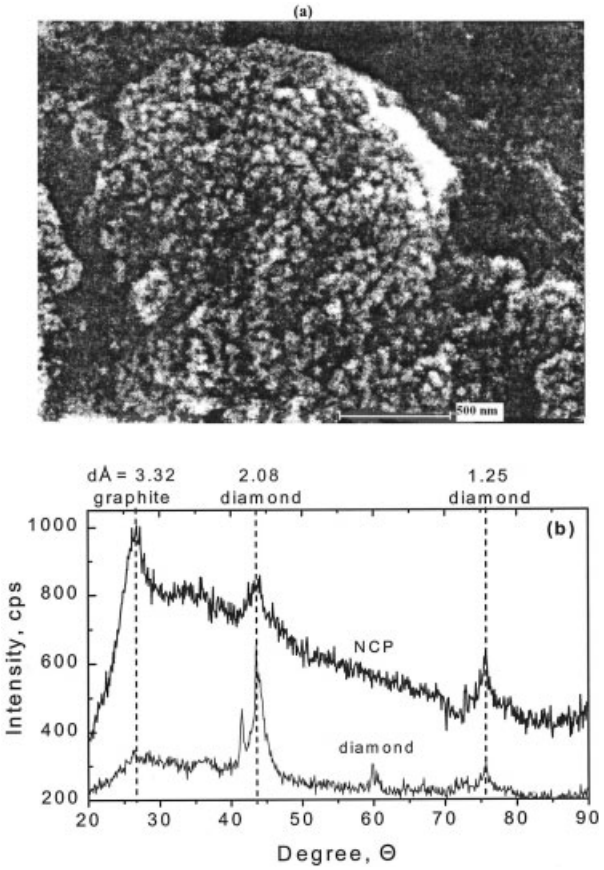

Figure 1. (a) Scanning electron micrograph of NCPs (data from ref. 37) with a micrometer bar of 500 nm. Small inclusions with an average diameter of approximately 10 nm and a maximum diameter of approximately 50 nm formed large clusters ranging from 200–1200 nm. (b) XRD spectra of NCPs and diamond.

Rheological Measurements

The rheological characteristics of the carbon/epoxy dispersions were measured with a Rheotron Brabender viscometer with cone–plate geometry. Steady-state shear measurements were carried out in the shear rate ($\dot{\gamma}$) region of 0.1–100 s^{-1}. The oscillatory shear mode in the frequency range of 0.1–75 s^{-1} at a low strain amplitude of 0.01% was used to measure the dynamic storage modulus (G') and loss modulus (G'') within the linear viscoelastic range. The relaxation time spectrum was calculated from the linear theory of viscoelas-

Table 1. Compositions and Characteristic Parameters of the Carbon/Epoxy Dispersions

	Carbon			
Sample	wt %	vol %	τ_m(s)	τ_m^{rel}
ER	0	0	0.12	1
1% NCP	1.68	1	0.12	1
2% NCP	3.34	2	0.14	1.17
4% NCP	6.58	4	0.16	1.33
6% NCP	9.74	6	0.33	2.75
8% NCP	12.82	8	1.03	8.58
10% NCP	15.82	10	5.82	48.5

ticity through the fitting of the experimental values of $G'(\omega)$ and $G''(\omega)$ (where ω is the angular frequency) to a generalized Maxwell model (eqs 1 and 2)[38] in terms of the relaxation spectrum coefficients, according to the Maxwell model (G_i and τ_i). The mean relaxation time (τ_m) was calculated from the relaxation spectrum coefficients (eq 3). Finally, the relative increase in the mean relaxation time (τ_m^{rel}) was determined as the ratio of the mean relaxation time of the nanodispersions [$\tau_m(\Phi > 0)$, where Φ is the volume fraction of carbon] to the mean relaxation time of matrix polymer [$\tau_m(\Phi = 0)$; eq 4]. τ_m^{rel}, the additional relaxation, was produced by the presence of the nanoparticles in the dispersions:

$$G'(\omega) = \sum_{i=1}^{n} G_i \omega^2 \tau_i^2 / (1 + \omega^2 \tau_i^2) \quad (1)$$

$$G''(\omega) = \sum_{i=1}^{n} G_i \omega \tau_i / (1 + \omega^2 \tau_i^2) \quad (2)$$

$$\tau_m = \sum_{i=1}^{n} G_i \tau_i^2 / \sum_{i=1}^{n} G_i \tau_i \quad (3)$$

$$\tau_m^{rel} = \tau_m(\Phi > 0)/\tau_m(\Phi = 0) \quad (4)$$

Both Rheometric software and a similar previously developed and proved method[39] were used for the calculation of the relaxation spectrum, τ_m, and τ_m^{rel}.

DSC

DSC temperature scans were taken of the samples after curing with a PerkinElmer DSC-7. Samples (ca. 1 mg) were sealed in aluminum pans and heated from 0 to 300 °C at scanning rate of 10 °C/min under a nitrogen atmosphere. The glass-transition temperature (T_g; onset) was determined from the curves with data from the second run.

Dielectric Measurements

With DRS analysis, the complex dielectric permittivity ($\epsilon = \epsilon' - i\epsilon''$, where ϵ' is the dielectric constant and ϵ'' is the dielectric loss) was measured as a function of frequency (10^{-2}–10^6 Hz) and temperature (from ca. −150 to ca. 200 °C).[17–20] A Schlumberger FRA SI 1260 frequency response analyzer, supplemented with a buffer amplifier of variable gain (Chelsea Dielectric Interface) and a Hewlett–Packard Precision HP4284A LCR meter, in combination with the Novocontrol Quatro Cryosystem, was used. Each sample was clamped between gold-plated, stainless steel electrodes in a Novocontrol dielectric cell. TSDC is a dielectric technique in the temperature domain and is complementary to DRS. It consists of recording the thermally activated release of frozen-in polarization and corresponds to the measurement of ϵ'' as a function of temperature at constant low frequencies in the range of 10^{-2}–10^{-4} Hz.[17,19]

Dynamic Mechanical Analysis (DMA)

The dynamic mechanical characteristics of solid composites—the storage modulus (E'), loss modulus (E''), and tan δ—were determined on a Rheometric Scientific DMTA IV dynamic mechanical thermal analyzer at strain amplitude of 0.2%, which was found to be the linear viscoelastic range for the solid epoxy composites studied. The cured samples were clamped in a medium frame with a small center clamp in the bending mode. A frequency of 1 Hz was used. The measurement temperature ranged from 23 to 300 °C; the heating rate was controlled at 2 °C/min.

RESULTS AND DISCUSSION

Rheological Properties of the Nanodispersions

Experimental and theoretical studies of colloidal dispersions predict that with increasing inorganic content, an aggregation of colloidal particles will take place, and this will lead to the formation of clusters of aggregates (fractal flocs) and finally to

an infinite cluster (network).[11,12] Dispersions of nanoparticles differ from classical colloidal dispersions by a much smaller mean interparticle distance, and the interparticle interaction is much more difficult to control.[10] Therefore, interactions between carbon nanoparticles cannot be neglected, and the preparation of well-defined systems requires strong control of the dispersion microstructure.

The studied carbon/epoxy dispersions obviously have a broad size distribution of particles, which range from nanosized single particles of a few nanometers to clusters of a micrometer size. As already postulated by Flandin and Schueler[1(a,b)] and measured by Harbourg et al.,[1(c)] carbon particles possess a permanent electrical charge that leads to a long-range Coulombic repulsion and thus results in an electrostatic stabilization of dispersions. The level of the potential barrier depends on the electric charge at the surface of the particles and on the polarity of the matrix. The shearing during mixing lowers this barrier. Thus, shearing and thermal agitation during high-power ultrasonic dispersion lead to the following two effects in epoxy/carbon dispersions. First, the NCP clusters disperse into smaller ones or single particles. Second, the motion of the dispersed particles in the medium and the collisions created by this motion involve sufficient energy to overcome the electrostatic barrier; therefore, pairs of particles become aggregated.

To characterize the nature of the microstructure and the evolution of the structural change of the carbon nanoparticle dispersion in shear flow, we adopt the concept of cluster–cluster aggregation in colloidal dispersions, which yields self-similar structures known as fractals.[11–14] Simulation studies[11,12] suggest that colloidal aggregates behave as stochastic mass fractals on a scale that is large in comparison with the primary particle size. In ref. 13, it is shown that clusters of submicrometer spheres, formed by rapid aggregation, form a network at a critical volume fraction (Φ^*) of approximately 0.05 (~5 vol %). The rheological properties of such aggregated dispersions are changed at Φ^*. Below Φ^*, dispersions are weakly shear-thinning and show little or no viscoelasticity. Above Φ^*, solid-like behavior is observed, and so data for the shear modulus (G) and yield stress (τ_0) suggest that aggregate networks show universal behavior that is consistent with the scalings $G \sim \Phi^{\mu}$ and $\tau_0 \sim G(\Phi)$. The theoretical values of scaling exponent μ are predicted to be 4.5 ± 0.2 under the assumption that the clusters comprising the network are fractal. For diffusion-limited aggregation, μ becomes 3.5 ± 0.2.[12,13]

Rheological measurements have been performed, which are informative for analyzing the structure of the carbon epoxy dispersions and the interaction between the particles. We have applied an oscillatory flow rheological technique under a small strain amplitude so that the structure of the dispersion is not much disturbed from its equilibrium conditions. Figure 2(a) shows that the carbon loading of a very low volume fraction reduces the terminal slope of the low-amplitude storage modulus from the theoretical value of $G' \sim \omega^2$ (for the pure resin) to $G' \sim \omega^{1.5}$ and $G' \sim \omega^{0.9}$ for 1 and 2% NCP/epoxy, respectively. Moreover, in the volume fraction range of 4–10%, $G'(\omega)$ trends to an equilibrium plateau in the terminal region, and this could be related to the formation of a network structure. Figure 2(b) presents the shear-flow data [shear stress ($\tau^{1/2}$) vs $\dot{\gamma}^{1/2}$] for the

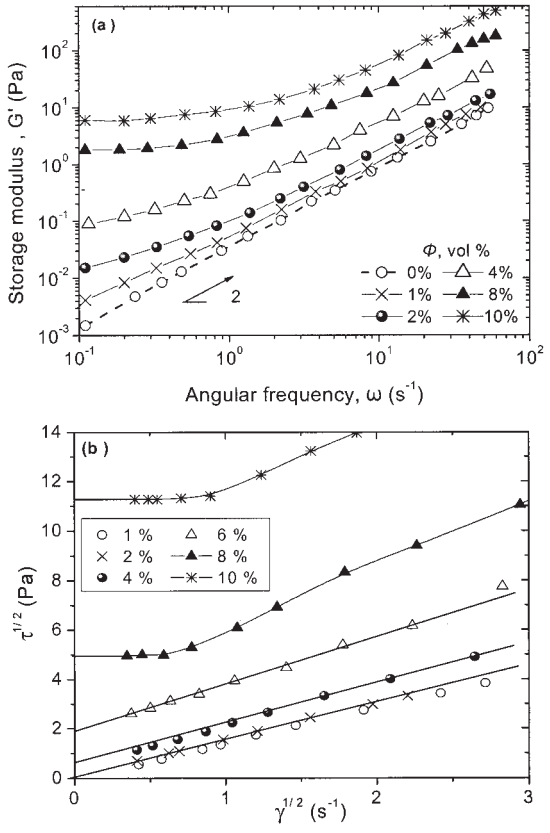

Figure 2. (a) Low-amplitude G' values versus ω and (b) Casson plot of $\tau^{1/2}$ versus $\dot{\gamma}^{1/2}$ for the carbon/epoxy dispersions with various values of Φ (vol %). The experimental temperature was 20 °C.

carbon/epoxy dispersions, which have been analyzed with Casson's equation:[40] $\tau^{1/2} = \tau_0^{1/2} + \eta^{1/2}\dot{\gamma}^{1/2}$, where τ_0 is the Casson yield value. τ_0 appears if Φ increases above 4%. Thus, the results from Figure 2 confirm the transition of the rheological behavior of the carbon/epoxy dispersions with increasing Φ from weak shear thinning (1–2%) to a solid (4–10%).

The changes in the elasticity of the dispersion structure due to particle aggregation have been determined from a log–log plot of G' (at $\omega = 0.1\ s^{-1}$) and τ_0 versus Φ (Fig. 3). The values of τ_0 have been shifted by division by a factor of 10. Two distinct straight lines have been obtained over the Φ range of 1–10% with two power laws:

$$G' \sim \Phi^{3.7} \text{ at } 1\% > \Phi > 5\%$$

$$G' \sim \Phi^{6.45} \text{ and } \tau_0 \sim G'(\Phi) \text{ at } 5\% > \Phi > 10\% \quad (5)$$

The power-law behavior for both functions is a signature of fractal structures. The lower power in the first region, $\Phi < 5\%$, indicates a weak interaction between the carbon particles. In contrast, at $\Phi > 5\%$, the interaction becomes much stronger, and the power in Φ becomes larger. Therefore, cluster–cluster aggregation and network formation can be proposed at $\Phi > 5\%$. The cross point of the straight lines in Figure 3, obtained at $\Phi^* \sim 5\%$, is defined as the critical concentration, which presents the transition of the structure of the carbon/epoxy dispersions from a cluster type to a fractal (network) type.

Figure 3 shows that the observed value of $\mu = 6.45$ at $\Phi > \Phi^*$ is higher than the theoretical values of $\mu = 4.5 \pm 0.2$ predicted for a colloidal dispersion structure of a fractal type. High values of the slope, such as 6 and 10, are reported in refs. 9 and 13 for strongly flocculated dispersions. The high power in Φ for carbon/epoxy nanodispersions can be related to the strong interparticle interactions produced by the small particle size, as well as the interfacial interactions. Because of the extended surface area of the nanofiller in the volume range $\Phi > \Phi^*$, most of the matrix polymer is in the state of an interface layer surrounding nanoparticles. This bond polymer layer, having elasticity different than that of the bulk polymer, obviously dominates the overall elasticity of the individual fractal flocs and increases the scaling exponent. In our previous studies,[2–4] Φ^* has been associated with the percolation threshold (Φ_c) and has led to a sharp increase in the electrical conductivity.

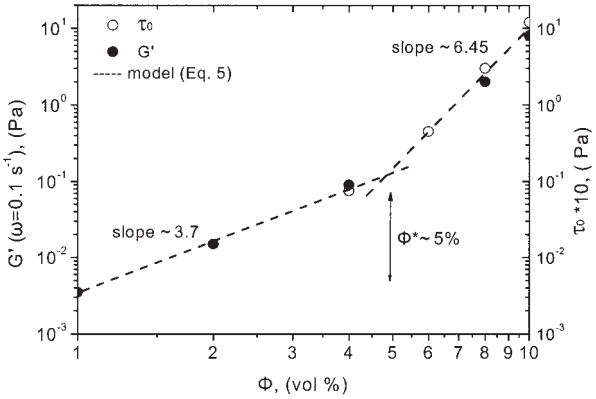

Figure 3. Plateau G' values (at $\omega = 0.1\ s^{-1}$) and τ_0 values (Casson) versus Φ of the epoxy dispersions at 20 °C. The values of τ_0 are divided by a factor of 10. The lines represent the prediction of the power-law model (eq 5). Slopes of 3.7 and 6.45 were determined for the two regions; the arrow shows $\Phi^* \sim 5\%$.

If the network structure of a dispersion is considered to be closely packed fractal flocs, according to Shih et al.,[14] the elasticity of the dispersion will be dominated by either interactions within flocs or interlinks between flocs. Such microstructural interactions in nanodispersions obviously produce an additional relaxation process, which can be clearly observed in the terminal flow region (Fig. 2). To describe quantitatively the additional relaxation processes in the nanodispersions, we use the linear theory of viscoelasticity to predict the relaxation in polymers through the calculation of the relaxation time spectrum.[38,39] Thus, the relaxation spectrum has been calculated from the experimental values of $G'(\omega)$ and $G''(\omega)$, in terms of G_i and τ_i, with eqs 1 and 2. Figure 4 compares the relaxation time spectra (G_i vs τ_i) of ER and carbon/epoxy dispersions with various filler concentrations of 2–10%. Table 1 shows the calculated values of τ_m and τ_m^{rel} (from eqs 3 and 4) at various carbon volume concentrations in the range of 1–10%.

With increasing filler content, the spectrum is shifted toward longer relaxation times. This is interpreted as a total characteristic for particle–particle and polymer–particle interactions, resulting in an additional relaxation behavior. The effect is strongly pronounced in the concentrated region (i.e., $\Phi > \Phi^*$), accounting for a restricted overall mobility of polymer chains in dispersions with respect to the pure epoxy matrix. Sharp increases in τ_m^{rel} (eq 4) can be observed above Φ^* with magnitudes of 2.75, 8.58, and 48.5 for the 6,

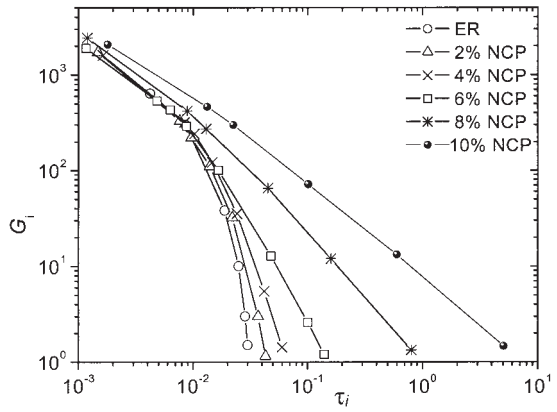

Figure 4. Relaxation time spectra of the carbon/epoxy dispersions with various carbon fractions at 20 °C.

8, and 10% NCP concentrations, respectively, if compared with a value of 1 for pure ER. We assume that such a strong increase in τ_m^{rel} is due to the formation of a network of interacted fractal flocs at high filler concentrations (8–10% NCP). As the fractal flocs consist of clusters of nanoparticles surrounded by an interface polymer layer, they behave as an elastic barrier during the shear flow and relax for a longer time than the matrix in the bulk. The alteration of the relaxation processes has also been observed in polymer/layered-silicate nanocomposites[15,16] and has been attributed to the end tethering of polymer segments at the silicate surfaces.

Molecular Dynamics of the Nanocomposites

The cured carbon/epoxy nanocomposites were examined with DSC, DRS, and TSDC techniques to evaluate the effects of the nanofillers on the molecular mobility of the polymeric chains and, in particular, on the cooperative motion of the chain segments at the interfaces.

Figure 5 compares the DSC thermograms of the cured ER and carbon/epoxy nanocomposites, and Table 2 presents the DSC data of T_g (onset). As shown in Figure 5, the DSC curve of pure ER shows a T_g (onset) at approximately 94 °C. The addition of the carbon nanofiller (2–6%) increases T_g by about 5–10 °C in comparison with T_g of pure ER. That confirms the assumption drawn from the rheological data, showing that the polymer chains must be under constraint because of the influence of the interfacial polymer–particle interactions; therefore, T_g of the nanocomposites has been shifted to higher temperatures. Such an increase in T_g has been discussed by other authors[16,30,31] in terms of an interface layer (bound polymer) around the filler particles due to chains being tied down by the inorganic surface. Our results clarify that above Φ^*, the change in T_g can be significant, as most of the polymer is immobilized as an interface layer around the particles, and so the interfacial effects dominate the bulk properties of the material.

Taken in the context of the restricted polymer relaxation in nanodispersions (Fig. 4) and the increased T_g values of the nanocomposites (Fig. 5), the results appear to indicate that the cooperative motion precipitously decreases because of the presence of nanoparticles. The effects observed here can be associated with the formation of a dense network, but it is an open question whether the curing reaction of ER is affected by the presence of carbon nanoparticles. Some results for nanocomposites suggest that the rate of reaction may change with the presence of modified nanolayers, but the final state of curing does not. For example, organically modified clay surfaces in clay/epoxy systems act primarily as acid catalysts rather than as curing agents.[41] The carbon nanoparticles probably act as additional crosslinks through the interface (bond) polymer layer, but the conditions of curing followed here with nonmodified carbon nanoparticles allow ER to achieve the final state of curing. It is not easy to separate the two effects; however, the morphology of the epoxy matrix at the interfaces could be affected by the nanofiller surfaces.

Figure 6 shows results obtained by DRS: ϵ' and ϵ'' versus the temperature for the pure ER matrix

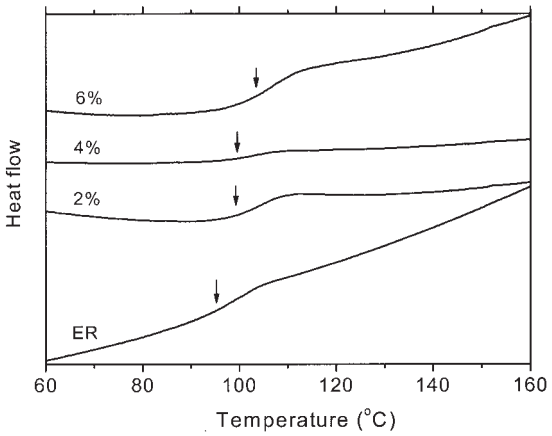

Figure 5. DSC thermograms of pure ER and carbon nanocomposites with different filler volume fractions. The arrows point out T_g (onset).

Table 2. DSC and DMA Summary of the Carbon/Epoxy Composites

Sample	T_g (Onset, °C)	T_α (°C)	Tan δ Peak	E' (MPa) 30 °C	80 °C	106 °C	150 °C
ER	94.0	104.6	1.062	2650	1130	56	20.7
2% NCP	98.6	104.6	0.903	2742	1490	117	32.7
4% NCP	99.0	106.7	0.927	3230	1610	138	31.4
6% NCP	103.9	108.6	0.816	2887	1900	290	67.6

and three nanocomposites at a constant frequency of 80,805 Hz. The data have been recorded isothermally by frequency scanning and have been replotted here to facilitate a comparison with DSC and dynamic mechanical data. A relatively high frequency has been chosen for the presentation to eliminate conductivity effects present at lower frequencies.[17] An overall increase of the molecular mobility can be observed in Figure 6 (in agreement with TSDC data not shown here), in the sense that, at each temperature, ϵ' and ϵ'' increase with increasing filler content. This is to a large extent related to the formation of a percolation structure of the nanoparticles, as confirmed by the dependence of ϵ' (at a frequency of 1 Hz and a temperature of −50 °C) on Φ of NCP in the inset of Figure 6(a). The well-known equation for the dependence of ϵ' on Φ from percolation theory has been used:[1]

$$\epsilon'(\Phi) = \epsilon_m' + A|\Phi - \Phi_c|^{-t} \qquad (6)$$

where ϵ_m' is the dielectric constant of the matrix and t is the critical exponent. The values of Φ_c and t have been determined to be 7.4% and 0.69, respectively.

Two relaxations, a secondary (β) relaxation at lower temperatures and a primary (α) relaxation at higher temperatures, associated with the glass transition of the ER matrix, can be observed in Figure 6.[17] For both relaxations, the strength [i.e., the magnitude of the peak in $\epsilon''(T)$ and the corresponding step in $\epsilon'(T)$] increases in the nanocomposites, particularly for the sample above Φ^*. The timescale (temperature position) of the response shows, however, a different behavior. For the local β relaxation, it does not change with the composition, whereas for the cooperative α relaxation, the peak temperature increases slightly in the nanocomposites, particularly at higher filler contents, at which it shifts out of the temperature range of Figure 6 (measurements at higher temperatures and lower frequencies are less conclusive for higher content nanocomposites, as the results are masked by conductivity effects). Thus, the DRS results allow us to discuss molecular mobility in terms of the relaxation strength and the timescale of the response. The increase in the

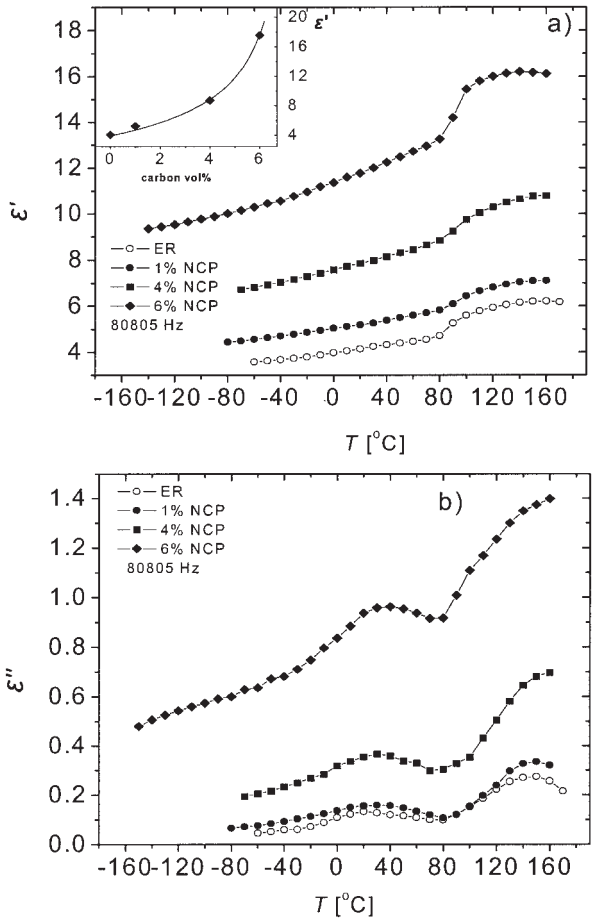

Figure 6. (a) Real part (ϵ') and (b) imaginary part (ϵ'') of the dielectric permittivity versus the temperature (T) at 80,805 Hz. The inset shows ϵ' (measured a 1 Hz and −50 °C) versus the NCP volume concentration. The line is a fit of eq 6 to the data.

relaxation strength for both β and α can be understood in terms of increased free volume, in agreement with results obtained for other nanocomposites.[17] The slowdown of the cooperative α relaxation (dynamic glass transition) provides additional evidence for the immobilization of polymer chains in the interface layer around the particles (the formation of a bound polymer).

The dynamics of the dielectric relaxations can be further studied on the basis of the Arrhenius plot (activation diagram) shown in Figure 7. The results in this figure refer only to dipolar relaxations. Conductivity effects have been eliminated by the fitting of an appropriate expression to the dielectric data after common praxis in the analysis of the dielectric measurements.[19,20] For the β relaxation, the results show that, although the timescale of the response does not change with the composition, the dynamics do change: the activation energy in the Arrhenius equation[19] decreases in the nanocomposites (0.69 eV in ER and 0.51, 0.59, and 0.63 eV in the nanocomposites with 1, 4, and 6% NCP, respectively), just like the corresponding frequency factor. The TSDC data, at the equivalent frequency of 1.6 mHz, corresponding to a relaxation time of 100 s,[19] are in good agreement with the DRS data for the two samples measured by both techniques and provide further support for the accuracy of the activation energy determination. For the α relaxation, for which less dielectric data are available with the required accuracy because of conductivity contributions, we show only the plot for the pure ER matrix with two DRS points, the DSC point (again at the equivalent frequency of 1.6 mHz[19]) and the point from dynamic mechanical measurements (to be discussed later). The Vogel–Tammann–Fulcher (VTF) equation,[17] which is characteristic for the α relaxation, has been fitted to the data. The fit is good (a broad frequency range is covered) with reasonable values of the fitting parameters and provides support for the consistency of the three techniques involved.

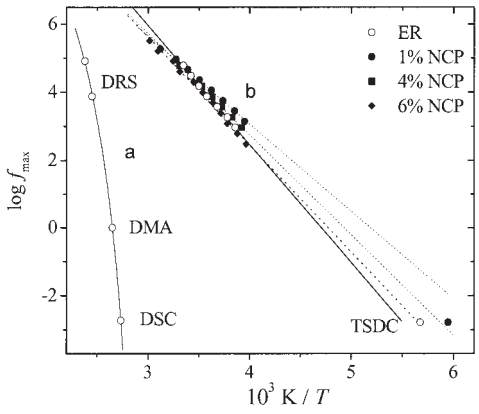

Figure 7. Arrhenius plot of (a) α and (b) β relaxations. The lines are fits of the VTF and Arrhenius equations, respectively, to the experimental data.

Dynamic Mechanical Properties

The effect of nanofillers on the viscoelastic properties of crosslinked (cured) epoxy matrix composites has been probed with DMA performed from 20 to 300 °C. This technique allows us to investigate the α relaxation, which is related to the Brownian motion of the main chains at the transition from the glassy state to the rubbery state, as explained previously with respect to molecular dynamics studies. It is likely that this motion can be affected by carbon nanofillers because of interactions in the interface layer around the particles. When a polymer goes through an α transition, tan δ shows a maximum at the α-transition temperature (T_α), and a substantial drop in E' and E'' appears, indicating viscous damping due to segmental motion in the polymer.[26] For crosslinked polymers, both E' and T_α generally increase with increasing crosslink density.[24,27]

Figure 8 shows the temperature dependence of E', E'', and tan δ of the ER matrix and carbon/epoxy composites with 2–6% NCP. Table 2 summarizes the most important dynamic mechanical data for the studied systems—T_α, tan δ, and E'—at 30 and 80, 106, and 150 °C, which represent three important regions: glassy, transition (glass to rubber), and viscoelastic (rubber), respectively. To compare the effects of the nanofiller in the three regions, the inset in Figure 8(a) presents the relative storage modulus (E'_{rel}), that is, the storage modulus of the nanocomposites divided by that of the pure resin, versus Φ at 80, 106, and 150 °C.

The presence of the nanofiller with 2–6% NCP enhances the values of E', and this effect appear in different magnitudes at various temperature ranges. As shown in Table 2 and by the intercept in Figure 8(a), $E'_{rel} = E'_{composite}/E'_{resin}$ is affected slightly by the nanofiller in the glassy region (30 – 80 °C), showing a 1.3–2 magnitude increase (~9%) for the composites over the pure epoxy. Above T_α, when materials become soft, the mechanical reinforcement by carbon nanoparticles becomes prominent. Notably,

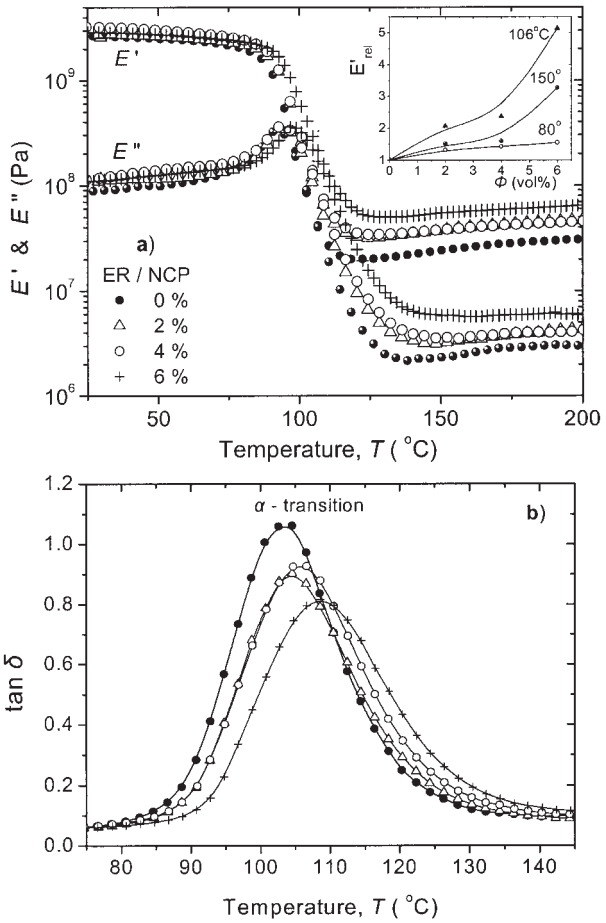

Figure 8. Dynamic mechanical behavior of the carbon/epoxy composites with various NCP concentrations (0, 2, 4, and 6%): (a) E' and E'' and (b) tan δ. The α transition is presented as the peak of the tan δ curves. The inset shows $E'_{rel} = E'_{composite}/E'_{resin}$ (measured at 80, 106, and 150 °C) versus the NCP volume concentration.

a significant increase in E' can be observed for nanocomposites with filler concentrations greater than Φ*. For example, 6% NCP/epoxy nanocomposites show an enhancement of E' of a magnitude of approximately 5.1 (420%) in the transition region (105 °C) and of a magnitude of 3.5 (226%) in the rubbery region (150 °C), in comparison with that of the pure resin. T_α also increases by a few degrees at this filler concentration, and this indicates an interface layer effect due to chains being tied down by the surface of carbon. Obviously, the network structure of such composites gives rise to better modulus reinforcement because the fractal flocs act as large soft particles during the deformation process. Typically, conventionally prepared epoxy composites containing micrometer or larger filler particles do not exhibit substantial changes in E' at the filler volume concentrations below 10–15 vol %.[29,30]

In addition, Figure 8(b) shows the tan δ results at 70–150 °C and estimations of the peak characteristics. The results summarized in Table 2 show that the tan δ peak decreases and becomes broader with increasing filler content, and this indicates that the chain mobility of the crosslinked epoxy is restricted by the presence of NCPs. The reduction of the tan δ peak is consistent with the increase in T_g noted in the DSC data (Table 2), and this effect becomes significant above Φ*, accounting for a structure with increased density.

In general, a microstructure consisting of fractal flocs, which is formed above Φ*, is proposed to play the main role in the reinforcement of nanocomposites. The interface polymer layer (bond layer), surrounding nanoparticles within the flocs, increases the relaxation strength and slows down the cooperative α relaxation and thus probably results in enhanced elasticity in both the transition and rubbery regions.

CONCLUSIONS

We have used the rheological approach for colloidal systems and have studied the scaling and relaxation behavior of carbon/epoxy nanodispersions. On the basis of the rheological results, the microstructure of the dispersions has been found to change from a cluster to a network (fractal) at $\Phi^* \sim 5$ vol %. G' and τ_0 (Casson value) scale above Φ* with $\mu = 6.45$, which is higher than the theoretical predictions for colloidal dispersions. This is associated with the small size of the carbon particles producing strong interparticle and interfacial interactions.

The rheologically determined microstructure of the dispersions is very important for the properties of the solid nanocomposites. The cooperative motion of the matrix polymer precipitously decreases in the presence of a nanofiller, and this results in an increase in T_g.

The results for the molecular dynamics from the dielectric measurements show that the relaxation strength of both the β and α relaxations increases in the nanocomposites, with respect to the pure polymer matrix. This is attributed to the increase in the free volume due to the loosened molecular packing of the polymer chains. The

timescale of the local β relaxation does not change in the nanocomposites, but the activation energy of the relaxation decreases. The cooperative α relaxation, on the other hand, slows down in the nanocomposites, being more pronounced at concentrations above Φ^*. This is explained by the larger characteristic length scale of that relaxation, which becomes comparable to the thickness of the polymer layer confined between the nanoparticles.

The network structure of fractal flocs above Φ^*, at which a large amount of the polymer is adsorbed at the particle surface, plays an important role in the reinforcement of nanocomposites. The overall composite elasticity above Φ^* increases significantly in the transition and rubbery regions, accounting for the dominant role of the elasticity of fractal flocs and interlinks between flocs. Such a hybrid structure produces a complex debonding process, easily undergoes deformation, and improves the stiffness of nanocomposites in the temperature region above the glass transition.

R. Kotsilkova thanks Venture Business Laboratory (VBL), Yamagata University (Japan), and K. Koyama for their partial support. Financial support by the Thales program of the National Technical University of Athens is also acknowledged.

REFERENCES AND NOTES

1. (a) Flandin, L.; Prasse, T.; Schueler, R.; Schulte, K.; Bauhofer, B.; Cavaille, J. Y. Phys Rev B 1999, 59, 14349; (b) Shueler, R.; Petterman, J.; Schuilte, K.; Wentzel, H. J Appl Polym Sci 1997, 63, 1741; (c) Harbourg, J. R.; Walzak, M. J.; Veregin, P. J Colloid Interface Sci 1990, 138, 380.
2. Kotsilkova, R.; Nesheva, D.; Nedkov, I.; Krusteva, E.; Stavrev, S. J Appl Polym Sci 2004, 92, 615.
3. Kotsilkova, R.; Krusteva, E.; Nesheva, D.; Djunova, S.; Stavrev, S. In Nanosciences and Nanotechnology: Nanostructured Materials Application and Innovation Transfer; Balabanova, E.; Dragieva, I., Eds.; Heron: Sofia, Bulgaria, 2003; Vol. 3, p 169.
4. Kotsilkova, R.; Krusteva, E. Proceedings of the 6th European Conference on Rheology, LSP-FAU, Erlangen, Germany, 2002; Münstedt, H.; Kashta, H.; Merten, J., Eds.; p 99.
5. Principles of Colloid and Surface Chemistry; Hiemenz, P. C., Ed.; Marcel Dekker: New York, 1986; Chapter 4.
6. Tardos, T. F. Langmuir 1990, 6, 28.
7. Clusters and Colloids; Schmid, G., Ed.; VCH: Weinheim, 1994.
8. Bousmina, M.; Muller, R. J Rheol 1993, 37, 663.
9. Steinmann, S.; Fahrlander, M.; Frassdorf, W.; Friedrich, C. Proceedings of the 13th International Congress on Rheology, Binding, D.M., Ed., Cambridge, England, 2000; Vol. 1, p 197.
10. Pelster, R.; Simon, U. Colloid Polym Sci 1999, 277, 2.
11. Meakin, P. Phys Rev Lett 1983, 51, 1119.
12. Kolb, M.; Botet, R.; Julien, R. Phys Rev Lett 1983, 51, 1123.
13. (a) Buscall, R.; Mills, P.; Coogwin, J.; Lawson, D. J Chem Soc Faraday Trans 1988, 1, 4249; (b) Buscall, R.; Mills, P.; Yates, G. E. Colloids Surf 1986, 18, 341.
14. Shih, W.-H.; Shih, W. Y.; Kim, S.; Liu, J.; Aksay, I. Phys Rev A 1990, 42, 4772.
15. Krishnamoorti, R.; Giannelis, E. Macromolecules 1997, 30, 4097.
16. Kotsilkova, R. Mechanics Time Dependent Materials; Kluwer Academic: Boston, 2002, 6, 283.
17. Vaia, R. R.; Giannelis, E. Chem Mater 1996, 8, 1728.
18. Bershtein, V. A.; Egorova, L. M.; Yakushev, P. N.; Pissis, P.; Sysel, P.; Brozova, L. J Polym Sci Part B: Polym Phys 2002, 40, 1056.
19. Kanapitsas, A.; Pissis, P.; Kotsilkova, R. J Non-Cryst Solids 2002, 305, 204.
20. Pissis, P.; Kanapitsas, A.; Georgoussis, G.; Bershtein, V. A.; Sysel, P. Adv Compos Lett 2002, 11, 40.
21. Mamunya, Y.; Kanapitsas, A.; Pissis, P.; Boiteux, G.; Lebedev, E. Macromol Symp 2003, 198, 449.
22. Fragiadakis, D.; Pissis, P.; Elie, C.; Kanapitsas, A.; Kotsilkova, R.; Stavrev, S.; Nedkov, I. Proceedings of the 10th International Conference on the Mechanics and Technology of Composite Materials, BAS, Sofia, Bulgaria, 2003; p 45.
23. Friedrich, K.; Karson, U. A. Fibre Sci Technol 1983, 18, 34.
24. Nicolopian, S. N.; Friedman, M. L.; Stalnova, U.; Popov, V. Adv Polym Sci 1990, 96, 1.
25. Kim, G. M.; Lee, D. H.; Hoffmann, B.; Kressler, J.; Stöppelmann, G. Polymer 2001, 42, 10095.
26. Friedrich, C.; Scheuchenpflug, W.; Neuhäusler, S.; Rösch, J. J Appl Polym Sci 1995, 57, 499.
27. Reynaud, E.; Jouen, T.; Gauthier, C.; Vigier, G.; Varlet, J. Polymer 2001, 42, 8759.
28. Shen, Y.; Finot, M.; Needlman, A.; Suresh, S. Acta Mater 1994, 42, 77.
29. Becker, C.; Krug, H.; Schmidt, H. Mater Res Soc Symp 1996, 435, 237.
30. Controlled Interphases in Composite Materials; Isida, H., Ed.; Elsevier: New York, 1990.
31. Molecular Characterization of Composite Interfaces; Isida, H.; Kumar, G., Eds.; Plenum: Seattle, 1983.
32. Chen, J.-S.; Poliks, M.; Ober, C.; Zhang, Y.; Wesner, U.; Gianellis, E. Polymer 2002, 43, 4895.

33. Tsagaropoulos, G.; Eisenberg, A. Macromolecules 1995, 28, 6067.
34. Berriot, J.; Montes, H.; Lequeux, F.; Long, D.; Sotta, P. Macromolecules 2002, 35, 9756.
35. Arrighi, V.; McEwen, I. J.; Qian, H.; Serrano Prieto, M. B. Polymer 2003, 44, 6259.
36. Stavrev, S. U.S. Patent 5,353,708, 1994.
37. Stavrev, S.; Kotsilkova, R.; Karadjov, J.; Karagyosova, Z. In Nanoscience and Nanotechnology: Nanostructured Materials Application and Innovation Transfer; Balabanova, E.; Dragieva, I., Eds.; Heron: Sofia, Bulgaria, 2001; Vol. 1, p 154.
38. Ferry, J. D. Viscoelastic Properties of Polymers; Wiley: New York, 1980; pp 1–80.
39. Kotsilkova, R.; Delchev, K.; Karastanev, S. J Physico-Chem Mech 2000, 25, 62.
40. Casson, N. In Rheology of Disperse Systems; Hill, C. C., Ed.; Pergamon: Oxford, 1959; p 84.
41. Wang, M. S.; Pinnavaia, T. Chem Mater 1994, 6, 468.